LETTERS

Friction laws at the nanoscale

Yifei Mo[1], Kevin T. Turner[1,2,3] & Izabela Szlufarska[1,3]

Macroscopic laws of friction do not generally apply to nanoscale contacts. Although continuum mechanics models have been predicted to break down at the nanoscale[1], they continue to be applied for lack of a better theory. An understanding of how friction force depends on applied load and contact area at these scales is essential for the design of miniaturized devices with optimal mechanical performance[2,3]. Here we use large-scale molecular dynamics simulations with realistic force fields to establish friction laws in dry nanoscale contacts. We show that friction force depends linearly on the number of atoms that chemically interact across the contact. By defining the contact area as being proportional to this number of interacting atoms, we show that the macroscopically observed linear relationship between friction force and contact area can be extended to the nanoscale. Our model predicts that as the adhesion between the contacting surfaces is reduced, a transition takes place from nonlinear to linear dependence of friction force on load. This transition is consistent with the results of several nanoscale friction experiments[4–7]. We demonstrate that the breakdown of continuum mechanics can be understood as a result of the rough (multi-asperity) nature of the contact, and show that roughness theories[8–10] of friction can be applied at the nanoscale.

According to the well-known Amontons' laws[11], formulated in 1699, the friction force F_f between two macroscopic bodies is linearly proportional to the applied load L, that is, $F_f = \bar{\mu}L$, where $\bar{\mu}$ is the macroscopic coefficient of friction. F_f is also independent of the macroscopic contact area A_{macro}. It was later noted[12] that a macroscopic contact is rough and consists of a large number of smaller contacts (so-called asperities), whose total area $\sum A_{asp}$ is much smaller than A_{macro}. The friction force was shown to be proportional to this true contact area, that is, $F_f = \bar{\tau}\sum A_{asp}$, where $\bar{\tau}$ is an effective shear strength of the contacting bodies (Table 1). To isolate surface roughness from other physical parameters that affect friction, many experiments and simulations have focused on studies of individual asperities, which have radii of curvature from tens of nanometres to micrometres in size and are assumed to be perfectly smooth[13–15]. Concurrently with single-asperity studies, roughness contact theories are being developed[8–10,16] to bridge the gap between the mechanics of single asperities and that of macroscopic contacts.

One reason single-asperity measurements have been so successful is that deformation of an asperity can be described by continuum mechanics theories (Table 1). A model for non-adhesive contact between homogenous, isotropic, linear elastic spheres, was first developed by Hertz[17], who showed that $A_{asp} \propto L^{2/3}$. Adhesion effects were included in a number of subsequent models, among which Maugis-Dugdale theory[18] has been frequently used because of its high degree of flexibility. The common feature of all the single-asperity theories is that A_{asp} is a sublinear function of L. In addition, several scanning force microscopy (SFM) studies have reported that $F_f = \tau A_{asp}$, with τ being an interfacial shear strength[13,19]. In this case, F_f will be a sublinear function of load[20].

A key question is whether single-asperity models can describe contact behaviour at the nanoscale. Deviations from single-asperity theories have sometimes been observed at these length scales and they have been attributed to the break-down of continuum mechanics. For instance, SFM experiments have been reported[5,6,21] where $F_f \propto L$ or even where these two quantities are nearly independent of each other[22]. More detailed discussion of the evidence for the break-down of continuum mechanics at the nanoscale can be found in ref. 13. The challenge in using SFM to establish friction laws at the nanoscale lies in the large sensitivity of contact behaviour to specific experimental conditions, such as surface chemistry or tip geometry. These challenges can be overcome in molecular dynamics simulations[1,5,20,23,24], which have been invaluable in identifying atomistic phenomena underlying friction. However, the use of idealized tip models or force fields in such molecular dynamics studies has led to contradictory results regarding friction laws. For instance, Luan and Robbins[1] and Wenning and Müser[25] found that for incommensurate non-adhesive contacts $F_f \propto L^{2/3}$, which was in contrast to later simulations by Gao *et al.*[20] who found $F_f \propto L$.

Here we perform large-scale molecular dynamics simulations of SFM experiments to determine friction laws at the nanoscale. We simulate

Table 1 | Summary of friction laws

Friction laws	F_f versus area	F_f versus L	Notes
Macroscale theories			
Amontons' law	Independent of A_{macro}	$F_f = \bar{\mu}\cdot L$	Law first discovered by Leonardo da Vinci
Bowden and Tabor	$F_f = \bar{\tau}\cdot\sum A_{asp}$	$F_f = \bar{\mu}\cdot L$	Law results from contact roughness
Single-asperity theories			
Non-adhesive (based on Hertz model)	$F_f = \tau\cdot A_{asp}$	$F_f \propto L^{2/3}$	Linear dependence of F_f on A_{asp} is generally believed to be true for microscale contacts, but has been questioned for nanoscale contacts
Adhesive (for example, Maugis–Dugdale)	$F_f = \tau\cdot A_{asp}$	Sublinear	
Multi-asperity picture of nanoscale contact (our model)			
Non-adhesive	$F_f = \tau\cdot A_{real} = \tau\cdot N_{at}\cdot A_{at}$ $F_f \neq \tau\cdot A_{asp}$	$F_f = \mu\cdot L$	Dependence of F_f on A_{real} has been directly verified. Linear dependence of F_f on L is due to atomic roughness and small contact pressures
Adhesive	$F_f = \tau\cdot A_{real} = \tau\cdot N_{at}\cdot A_{at}$ $F_f \neq \tau\cdot A_{asp}$	Sublinear	Adhesion induces transition from linear to sublinear behaviour

A_{macro} is the macroscopic contact area. A_{asp} is the contact area of a single asperity; A_{real} is the real contact area defined as the number of atoms N_{at} in contact multiplied by the average contact area A_{at} of an interfacial atom.

[1]Materials Science Program, [2]Department of Mechanical Engineering, [3]Department of Materials Science and Engineering, University of Wisconsin, Madison, Wisconsin 53706, USA.

sliding under a normal load and we determine the dependence of friction force on the applied load, contact area, and on the presence of adhesion at the interface. We focus on amorphous carbon tips and diamond samples (Fig. 1a), both terminated with hydrogen, because of the availability of experimental data[20] that can be used for comparison. We use realistic force fields[26], spherical tips that are allowed to deform together with the sample and that have curvature radii R of up to 30 nm (see Supplementary Fig. S1), and the simulations are performed at the temperature of 300 K. The force fields consist of short-range chemical interactions and long-range van der Waals interactions.

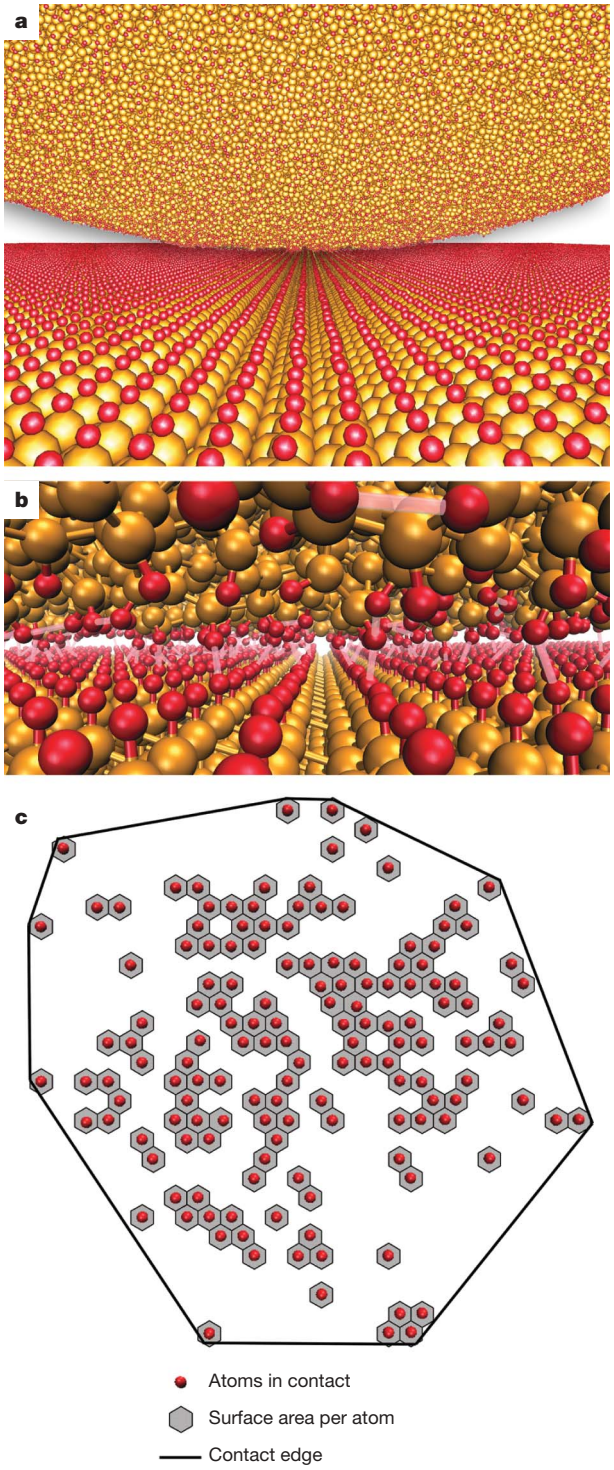

Figure 1 | Contact between an amorphous carbon tip and a diamond sample. a, Far view, showing contact geometry. Golden and red atoms correspond to C and H, respectively. **b**, Close view. Solid red and golden sticks represent covalent bonds. Translucent pink sticks represent repulsive interactions. **c**, Contact area definitions. Red circles represent sample atoms within the range of chemical interactions from tip atoms. Contact area per atom A_{at} is represented by grey hexagons. Real contact area A_{real} is the sum of the areas of hexagons. The contact area A_{asp} of an asperity is enclosed by the edge (solid line) of the contact zone.

Defining contact area is one of the major challenges for understanding friction in nanoscale contacts. Because fundamentally contact is formed by atoms interacting across the interface (Fig. 1b), we define a real contact area to be $A_{real} = N_{at}A_{at}$, where N_{at} is the number of atoms of the sample within the range of chemical interactions from the tip atoms and A_{at} is the average surface area per atom. In continuum mechanics A_{asp} is defined by the edge of the contact zone. The definition of the contact edge becomes ambiguous when the atomistic nature of the interface dominates its physical behaviour[27,28]. Here, we define A_{asp} to be the area enclosed by a convex hull around atoms in contact, as shown in Fig. 1c.

We first perform molecular dynamics simulations of normal loading and friction in the absence of van der Waals forces. Because both the tip and the sample are passivated with hydrogen atoms, adhesion due to short-range chemical forces is negligible. In this case a non-adhesive single asperity (Hertz) model is expected to apply, that is, $A_{asp} = \pi(3R/4E^*)^{2/3}L^{2/3}$, where $E^* = \left[\left(1-\nu_1^2\right)/E_1 + \left(1-\nu_2^2\right)/E_2\right]^{-1}$ is the effective modulus of the contact, E_1 and E_2 are the tip and the sample Young's moduli, and ν_1 and ν_2 are the tip and the sample Poisson's ratios, respectively. With the additional assumption of $F_f = \tau A_{asp}$, the Hertz model predicts that $F_f \propto L^{2/3}$. Our calculations show that $A_{asp} \propto L^{0.7}$ and $F_f \propto L$ (Fig. 2a), which yields $F_f \neq \tau A_{asp}$. Additionally, even though A_{asp} obtained in simulations shows approximately the same 2/3 power-law dependence on L as in the Hertz theory, the effective modulus E^* values calculated from fitting the Hertz model to the simulation data are 61% smaller than the value calculated directly from the definition of E^* (see Supplementary Methods). Our results confirm the conclusions of other authors that single-asperity theories break down at the nanoscale[1,5]. To account for the fact that F_f is not linear with A_{asp}, Wenning and Müser[25] suggested that τ is not a constant, but varies with contact pressure. Other authors proposed an empirical model in which mechanics of a nanoscale non-adhesive contact is controlled by load, that is, $F_f = \mu L$ and the contact area is undefined and unnecessary[5,29].

We argue that the break-down of single-asperity theories of friction is due to the fact that at these length scales the real contact area A_{real} is different from A_{asp} (see Fig. 1c) and that friction laws should be defined in terms of A_{real}. Our simulations show that $A_{real} \propto L$ (Fig. 2b) and $F_f = \tau A_{real}$ with constant τ (Fig. 2c), which is consistent with the relation $F_f \propto L$ (Fig. 2a). As shown in Table 1, friction force is now proportional to contact area at all length scales as long as the contact area is correctly defined at each length scale. Also, realizing that it is A_{real} (or, more fundamentally, N_{at}) that controls friction at the nanoscale, we can now understand why $F_f \propto L$. Such linear dependence is characteristic of rough contacts (Table 1) and in our case is a result of atomic roughness, as shown by the fact that $A_{real} \neq A_{asp}$. The above results demonstrate that a nanoscale contact, which had been previously viewed as a single entity, consists of yet smaller contacts of atomic size. Macroscale roughness theories can be applied to describe the behaviour of nanoscale contacts (see Supplementary Methods).

We investigate the effect of van der Waals adhesion on contact behaviour by adding these forces to the tip–sample interactions and by performing additional molecular dynamics simulations. As shown in Fig. 3a, the relation $F_f = \tau A_{real}$ still holds, which demonstrates that friction is controlled by the short-range (chemical) interactions even in the presence of dispersive forces. However, unlike the non-adhesive case, here F_f is a sublinear function of L (Fig. 3b), which is consistent with predictions of adhesive single-asperity models (see Table 1). We fit $F_f(L)$ to the Maugis–Dugdale model using a convenient approximation proposed by Carpick, Ogletree, and Salmeron (COS)[30] and later physically justified by Schwarz[31]. The fits show an excellent agreement with both

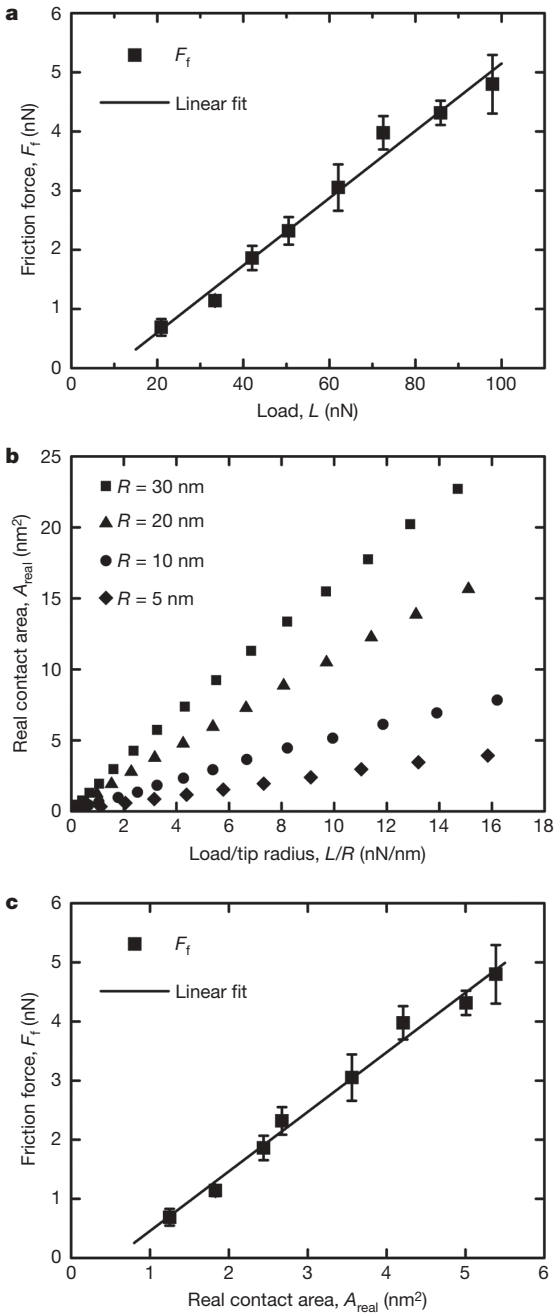

Figure 2 | Mechanics of non-adhesive contacts. **a**, Friction force versus load. **b**, Real contact area versus load. **c**, Friction force versus contact area. F_f is measured over five lattice periods of the sample's surface. The error bars in **a** and **c** correspond to a standard deviation in these measurements. Linear extrapolation to $F_f \rightarrow 0$ leads to finite values of A_{real} and L, but it is not clear whether such extrapolation should be linear. Measurements at very small loads carry large uncertainty owing to the small number of atoms in contact and to thermal vibrations.

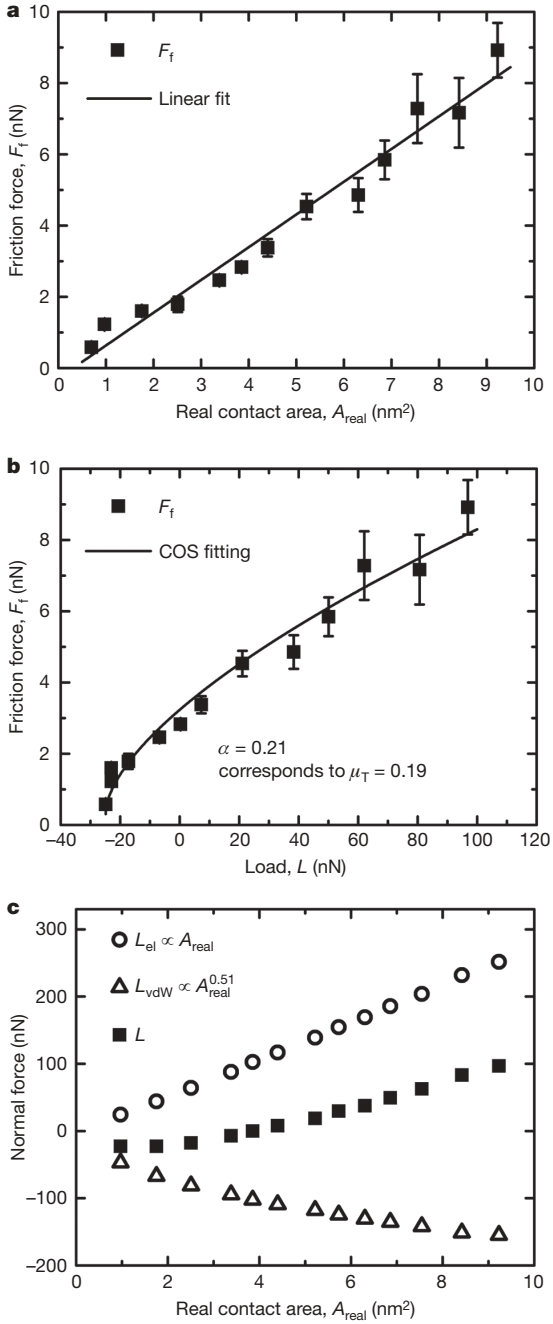

Figure 3 | Mechanics of adhesive contacts. **a**, Friction force versus real contact area. **b**, Friction force versus load. **c**, Contributions to the total load as a function of real contact area: total load L (full squares); van der Waals contribution L_{vdW} (empty triangles); elastic restoring force $L_{el} = L - L_{vdW}$ (empty circles). F_f is measured over three lattice periods of the sample's surface. The error bars in **a** and **b** correspond to a standard deviation in these measurements.

the Maugis–Dugdale theory and with experimental results (see Methods Summary), which validates our modelling approach. For instance, the fitted value of Tabor's[32] parameter μ_T is 0.19, which falls within the range of 0.11–0.22 calculated directly from theory for our system.

However, the fact that adhesive single-asperity theory fits both our simulation data and experimental data very well should not be taken as evidence that the theory represents the correct physics. We argue that the flexibility of the Maugis–Dugdale model (that is, three fitting parameters) masks the model's physical deficiencies. For instance, we can check whether the elastic restoring force L_{el}, calculated by subtracting van der Waals forces L_{vdW} from the total load L, follows Hertz's predictions, that is, whether $A_{real} \propto L_{el}^{2/3}$. As can be seen from Fig. 3c, $A_{real} \propto L_{el}$, which means that the correct physical picture is that of a rough (multi-asperity) contact rather than of a single-asperity one (see Table 1).

Why then does F_f depend sublinearly on L? This behaviour is due to the presence of adhesion forces L_{vdW}, which for a spherical tip in contact with a flat sample do not scale linearly with A_{real} (triangles in Fig. 3c). As a result the total load $L = L_{el} + L_{vdW}$ is not proportional to A_{real} and hence $F_f = \tau A_{real}$ is a sublinear function of L. Our models therefore predict that as adhesion in the contact is increased, a transition takes place from linear to sublinear dependence of F_f on L. The opposite effect can be achieved by increasing the roughness of the

interface. Behaviour consistent with single-asperity theories can be expected in the limit of $A_{real} \approx A_{asp}$, for example, for large contact pressures and for tip radii in the micrometre range and larger[9,33].

The identification of the multi-asperity nature of dry nanoscale contacts and of the associated laws of friction allows controversies that exist in the field to be resolved. For instance, the sublinear dependence of friction on load for non-adhesive incommensurate contacts reported by Luan and Robbins[1] is probably due to the relatively low roughness of the simulated interfaces. Two effects could contribute to this low surface roughness. First, the simulated surfaces were bare, that is, they were not passivated with adsorbate atoms. Second, the repulsive part of the Lennard–Jones force field that was used in the simulations is physically too stiff, which reduces corrugation of the surface potential energy. Low surface corrugation (roughness) results in $A_{real} \approx A_{asp}$, which explains why the authors observed a sublinear dependence of F_f on L. Gao *et al.*[20] simulated the opposite limit of contact behaviour. These authors used more realistic force fields and they simulated surfaces passivated with hydrogen atoms, which yielded atomically rough interfaces and resulted in the $F_f \propto L$ dependence. Atomic roughness was additionally frozen in by making the tip rigid. The transition from sublinear to linear $F_f(L)$ dependence due to adhesion reduction has been previously observed experimentally[4–6,34,35]. We can now understand that such transition takes place when contact roughness, defined by the corrugation of surface potential energy, becomes large in comparison to the range of interfacial interactions. Adhesion reduction can be realized for instance by surface passivation[6] or surface functionalization[4,34]. The transition from sublinear to linear friction can occur also during sliding if the surfaces are damaged (that is, roughened) in the process[5].

METHODS SUMMARY

In molecular dynamics simulations we use the reactive empirical bond-order (REBO) potential[26]. The REBO potential accurately describes the cohesive energies and chemical reactions of hydrocarbon systems as well as the elastic constants of solid carbon-based materials. The range of the REBO potential extends as far as the chemical interactions and does not include dispersive forces. The van der Waals interactions are therefore integrated with REBO using an analytical switching function in the regime where the two potentials overlap. For detailed description of the simulation techniques and schedule see Supplementary Methods.

We have also performed finite element analysis to demonstrate that the effect of boundary conditions in our simulations is negligible, that is, if our tips were represented by continuous, linear-elastic solids with smooth interfaces, the contact behaviour would be accurately described by continuum single-asperity models.

Our simulations show an excellent agreement with theory and experiments. For example, the F_f versus L dependence obtained in our simulations for an $R = 30$ nm adhesive tip sliding over H terminated diamond (111) surface was fitted to the Maugis–Dugdale model (see Supplementary Methods). The fitted COS transition parameter is 0.21, which yields the Tabor's[32] parameter μ_T of 0.19. Direct calculation of μ_T, based on our system geometry and elastic properties, gives a range from 0.11 to 0.22, which brackets the fitted value of μ_T. Our fits show that μ_T decreases with decreasing R, which is also in agreement with single-asperity models. Both the shear strength τ and the contact pressure are of the same order of magnitude as in SFM experiments[20]. Specifically, using a procedure similar to that in ref. 20 for $R = 30$ nm we estimate that $\tau \approx 508$ MPa and the contact pressure at $L \approx 100$ nN is 6.12 GPa.

Received 3 September; accepted 23 December 2008.

1. Luan, B. & Robbins, M. O. The breakdown of continuum models for mechanical contacts. *Nature* **435,** 929–932 (2005).
2. Delrio, F. W. *et al.* The role of van der Waals forces in adhesion of micromachined surfaces. *Nature Mater.* **4,** 629–634 (2005).
3. Zykova-Timan, T., Ceresoli, D. & Tosatti, E. Peak effect versus skating in high-temperature nanofriction. *Nature Mater.* **6,** 230–234 (2007).
4. Colburn, T. J. & Leggett, G. J. Influence of solvent environment and tip chemistry on the contact mechanics of tip-sample interactions in friction force microscopy of self-assembled monolayers of mercaptoundecanoic acid and dodecanethiol. *Langmuir* **23,** 4959–4964 (2007).
5. Gao, J. *et al.* Frictional forces and Amontons' law: from the molecular to the macroscopic scale. *J. Phys. Chem.* **108,** 3410–3425 (2004).
6. Grierson, D. S. *Nanotribological Properties of Nanostructured Hard Carbon Thin Films.* PhD thesis, Univ. Wisconsin (2008).
7. Ruths, M. Boundary friction of aromatic self-assembled monolayers: Comparison of systems with one or both sliding surfaces covered with a thiol monolayer. *Langmuir* **19,** 6788–6795 (2003).
8. Müser, M. H. A rigorous, field-theoretical approach to the contact mechanics of rough, elastic solids. *Phys. Rev. Lett.* **100,** 055504 (2008).
9. Persson, B. N. J. Theory of rubber friction and contact mechanics. *J. Chem. Phys.* **115,** 3840–3861 (2001).
10. Greenwood, J. A. & Williamson, J. B. P. Contact of nominally flat surfaces. *Proc. R. Soc. Lond. A* **295,** 300–319 (1966).
11. Amontons, G. De la resistance causée dans les machines. *Mem. Acad. R. A* 275–282 (1699).
12. Bowden, F. P. & Tabor, D. *The Friction and Lubrication of Solids* (Clarendon, 1950).
13. Szlufarska, I., Chandross, M. & Carpick, R. W. Recent advances in single-asperity nanotribology. *J. Phys. D* **41,** 123001 (2008).
14. Binnig, G., Quate, C. F. & Gerber, C. Atomic force microscope. *Phys. Rev. Lett.* **56,** 930–933 (1986).
15. Perry, S. S. Scanning probe microscopy measurements of friction. *MRS Bull.* **29,** 478–483 (2004).
16. Bush, A. W., Gibson, R. D. & Thomas, T. R. The elastic contact of a rough surface. *Wear* **35,** 87–111 (1975).
17. Hertz, H. On the contact of elastic solids. *J. Reine Angew. Math.* **92,** 156 (1881).
18. Maugis, D. Adhesion of spheres—the JKR-DMT transition using a Dugdale model. *J. Colloid Interface Sci.* **150,** 243–269 (1992).
19. Riedo, E., Chevrier, J., Comin, F. & Brune, H. Nanotribology of carbon based thin films: The influence of film structure and surface morphology. *Surf. Sci.* **477,** 25–34 (2001).
20. Gao, G. T., Cannara, R. J., Carpick, R. W. & Harrison, J. A. Atomic-scale friction on diamond: a comparison of different sliding directions on (001) and (111) surfaces using MD and AFM. *Langmuir* **23,** 5394–5405 (2007).
21. Pietrement, O. & Troyon, M. Study of the interfacial shear strength pressure dependence by modulated lateral force microscopy. *Langmuir* **17,** 6540–6546 (2001).
22. Socoliuc, A., Bennewitz, R., Gnecco, E. & Meyer, E. Transition from stick-slip to continuous sliding in atomic friction: Engineering a new regime of ultralow friction. *Phys. Rev. Lett.* **92,** 134301 (2004).
23. Chandross, M., Lorenz, C. D., Stevens, M. & Grest, G. S. Simulations of nanotribology with realistic probe tip models. *Langmuir* **24,** 1240–1246 (2008).
24. Szlufarska, I., Nakano, A. & Vashishta, P. A crossover in the mechanical response of nanocrystalline ceramics. *Science* **309,** 911–914 (2005).
25. Wenning, L. & Müser, M. H. Friction laws for elastic nanoscale contacts. *Europhys. Lett.* **54,** 693–699 (2001).
26. Brenner, D. *et al.* A second-generation reactive empirical bond order (REBO) potential energy expression for hydrocarbons. *J. Phys. Condens. Matter* **14,** 783–802 (2002).
27. Johnson, K. L. Adhesion and friction between a smooth elastic spherical asperity and a plane surface. *Proc. R. Soc. Lond. Ser. A* **453,** 163–179 (1997).
28. Luan, B. & Robbins, M. O. Contact of single asperities with varying adhesion: comparing continuum mechanics to atomistic simulations. *Phys. Rev. E* **74,** 026111 (2006).
29. Israelachvili, J. N. & Berman, A. D. in *Handbook of Micro/Nanotribology* (ed. Bhushan, B.) 2nd edn, 371–432 (CRC Press, 1999).
30. Carpick, R. W., Ogletree, D. F. & Salmeron, M. A general equation for fitting contact area and friction vs load measurements. *J. Colloid Interface Sci.* **211,** 395–400 (1999).
31. Schwarz, U. D. A generalized analytical model for the elastic deformation of an adhesive contact between a sphere and a flat surface. *J. Colloid Interface Sci.* **261,** 99–106 (2003).
32. Tabor, D. Surface forces and surface interactions. *J. Colloid Interface Sci.* **58,** 2–13 (1977).
33. Horn, R. G., Israelachvili, J. N. & Pribac, F. Measurement of the deformation and adhesion of solids in contact. *J. Colloid Interface Sci.* **115,** 480–492 (1987).
34. Ruths, M., Alcantar, N. A. & Israelachvili, J. N. Boundary friction of aromatic silane self-assembled monolayers measured with the surface forces apparatus and friction force microscopy. *J. Phys. Chem. B* **107,** 11149–11157 (2003).
35. Putman, C. A. J., Igarashi, V. & Kaneko, R. Single-asperity friction in friction force microscopy — The composite-tip model. *Appl. Phys. Lett.* **66,** 3221–3223 (1995).

Supplementary Information is linked to the online version of the paper at www.nature.com/nature.

Acknowledgements We thank D. Morgan for helpful discussions. Financial support from the National Science Foundation grant DMR-0512228 and from the American Chemical Society PRF-47978-G5 grant is gratefully acknowledged.

Author Contributions I.S. conceived the simulations and Y.M carried them out. Y.M. and I.S. designed the data analysis and Y.M. carried it out. I.S. and Y.M. co-wrote the paper. K.T.T. provided guidance and software for finite element analysis.

Author Information Reprints and permissions information is available at www.nature.com/reprints. Correspondence and requests for materials should be addressed to I.S. (izabela@engr.wisc.edu).